ELSEVIER

Optics Communications 146 (1998) 220–224

OPTICS COMMUNICATIONS

Photorefractive light amplification by forward four-wave mixing in $BaTiO_3$

J. Neumann [a,1], S. Mendricks [a], E. Krätzig [a], M. Goulkov [b], S. Odoulov [b,2]

[a] *Fachbereich Physik, Universität Osnabrück, Barbarastrasse 7, D-49069 Osnabrück, Germany*
[b] *Institute of Physics, National Academy of Sciences, 252 650 Kiev, Ukraine*

Received 21 July 1997; accepted 18 September 1997

Abstract

We demonstrate a new method of light amplification in photorefractive $BaTiO_3$. An ordinary signal beam is amplified by an extraordinary and an ordinary pump beam. A forward phase-conjugate beam is simultaneously generated. © 1998 Published by Elsevier Science B.V.

PACS: 42.65.Hw; 42.70.Nq
Keywords: Photorefractive effect; Phase conjugation; Four-wave mixing

1. Introduction

Many interesting holographic scattering phenomena have been found in photorefractive $BaTiO_3$ [1–6]. They are the results of 'noisy' volume phase gratings recorded by incident light waves and waves scattered from volume or surface imperfections of the crystal. Subsequently the scattered light is amplified because of direct coupling of two waves by a shifted grating (beam-fanning), or because of parametric mixing of more than two waves (parametric scattering). As a consequence of certain phase-matching conditions involved, these parametric processes may lead to characteristic scattering patterns.

Not only scattered waves, but also additional coherent light beams may be amplified by these processes. The case of two-beam coupling has been studied intensively [7–9] because of the wide range of applications, including real-time holography, coherent signal-beam amplification, and parallel signal processing. The beam-fanning adds a coherent optical background to the amplified signal beam, lowering the signal-to-background ratio.

In this Letter we report on the amplification of a signal beam by parametric mixing of four copropagating waves. The signal beam is amplified by two pump beams and simultaneously a forward phase-conjugate beam is generated. The corresponding scattering process has been already studied in Refs. [4,10,11]. Parametric holographic scattering processes based on the photorefractive effect have been considered for the enhancement of the signal-to-background ratio in two-wave mixing experiments [12] and to explain the coupling of orthogonally polarized waves [13]. But, to our knowledge, these parametric processes have not yet been used for the amplification of light beams.

2. Experiments

The experimental arrangement is shown schematically in Fig. 1(a). An ordinarily polarized pump wave with wavevector $\boldsymbol{k}_p^o$ and an extraordinarily polarized one with $\boldsymbol{k}_p^e$ of an Ar^+ ion laser ($\lambda = 514.5$ nm, intensity $I_p^o = I_p^e = 330\ \mathrm{mW/cm^2}$) impinge upon a $BaTiO_3$ sample symmetrically. The expanded beams (diameter 2 mm) form an angle $2\theta_p = 48°$ (measured in air) in the plane of incidence which is chosen perpendicular to the $\boldsymbol{c}$-axis of the sample. We use a $BaTiO_3$ crystal of dimensions 3.2 mm × 4.0

[1] E-mail: jens.neumann@physik.uni-osnabrueck.de.
[2] E-mail: odoulov@marion.iop.kiev.ua.

PII S0030-4018(97)00540-3

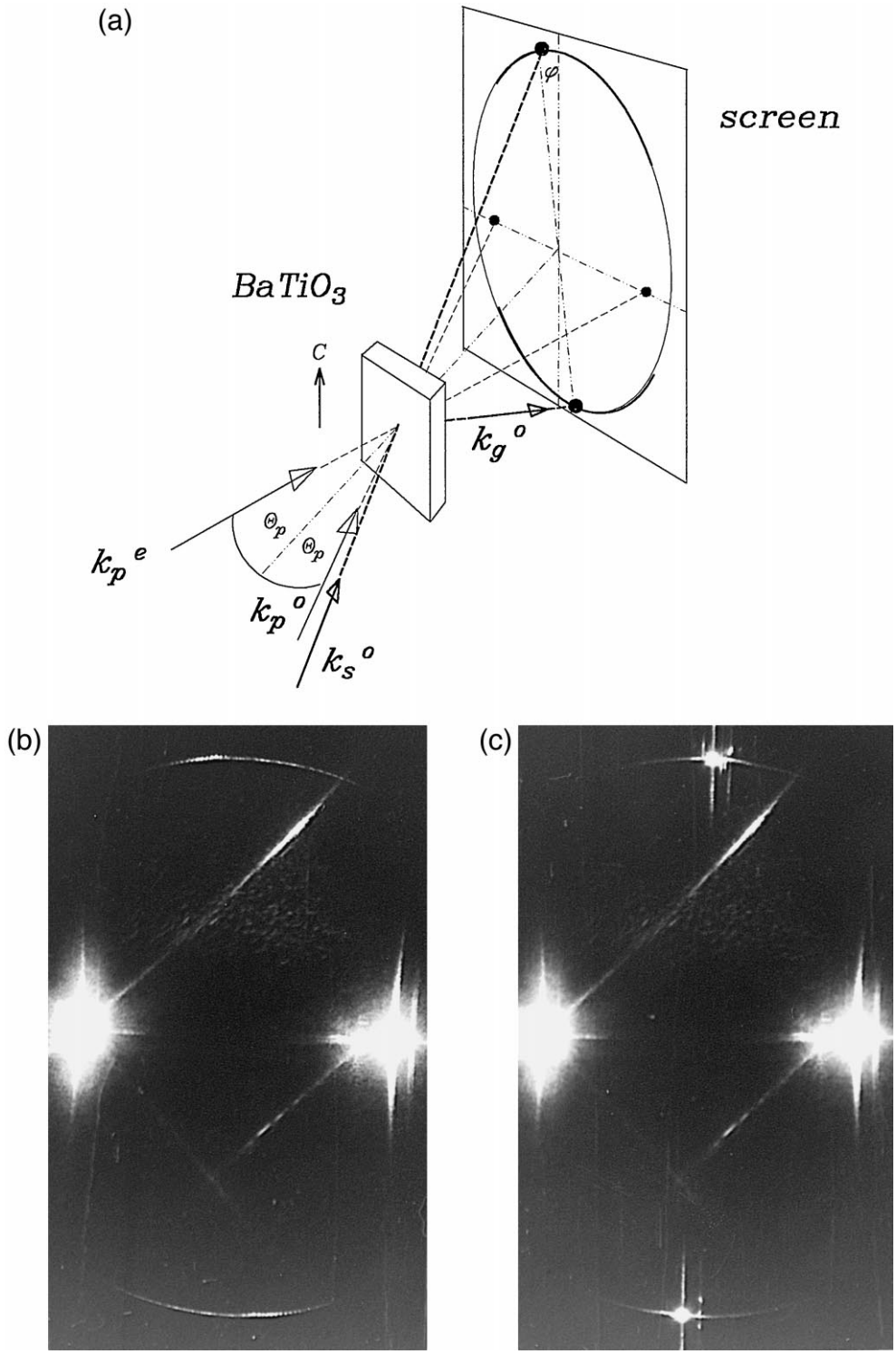

Fig. 1. (a) Experimental arrangement; $\boldsymbol{k}_{\mathrm{p}}^{\mathrm{o}}$ and $\boldsymbol{k}_{\mathrm{p}}^{\mathrm{e}}$ denote the wave vectors of the pump beams; $\boldsymbol{k}_{\mathrm{s}}^{\mathrm{o}}$ is the wave vector of the signal beam and $\boldsymbol{k}_{\mathrm{g}}^{\mathrm{o}}$ that of the generated beam (see text). (b) Scattering cone obtained on the screen behind the crystal. (c) When a signal beam propagates in the direction of the scattering cone an additional beam is generated also propagating on the scattering cone.

mm × 3.3 mm ($a \times b \times c$) cut along the principal crystal axes. The absorption coefficient for ordinary polarization at 514.5 nm is $\alpha = 2.5\ \mathrm{cm}^{-1}$. A third coherent ordinary beam with wavevector $\boldsymbol{k}_s^o$ is introduced as illustrated in Fig. 1(a). The intensity of this beam can be varied.

When only the two pump beams illuminate the crystal we observe on a screen placed about 1 m behind the sample the development of a scattering ring shown in Fig. 1(b). The light scattered into the cone has ordinary polarization. This scattering was discovered and studied in Refs. [4,10,11] and has been attributed to noise light amplification caused by the mixing of four copropagating waves obeying the phase matching condition $\boldsymbol{k}_p^o + \boldsymbol{k}_p^e = \boldsymbol{k}_1^o + \boldsymbol{k}_2^o$ inside the crystal. Here $\boldsymbol{k}_{1,2}^o$ are the wavevectors of the amplified scattered light waves on the cone.

To demonstrate the amplification of an additional coherent laser beam, we introduce the ordinary beam $\boldsymbol{k}_s^o$ (Fig. 1(a)). This beam is amplified inside the crystal, when it propagates in the direction of the scattering cone. In this case an additional ordinary beam ($\boldsymbol{k}_g^o$) is also generated (called generated beam in the following), propagating along the cone (Fig. 1(c)), too. The wavevectors involved fulfill inside the crystal the phase matching condition:

$$\boldsymbol{k}_p^o + \boldsymbol{k}_p^e = \boldsymbol{k}_s^o + \boldsymbol{k}_g^o . \qquad (1)$$

The solid lines in Fig. 2 represent the typical time evolutions of the transmitted signal beam intensity I_s for two different experiments (a) and (b): (a) At the beginning only the signal beam illuminates the crystal. When the pump beams are switched on (at t = 18 s) the signal beam grows in intensity until saturation is reached. (b) At the beginning of exposure only the two pump beams illuminate the crystal. Scattered light appears. It is responsible for the non-zero values of the signal beam intensity. When it has reached a stationary value the signal beam is switched on (at $t = 105$ s). It grows in intensity until the same saturation value is reached as in experiment (a). The dashed curves in Fig. 2 represent the intensity I_g of the

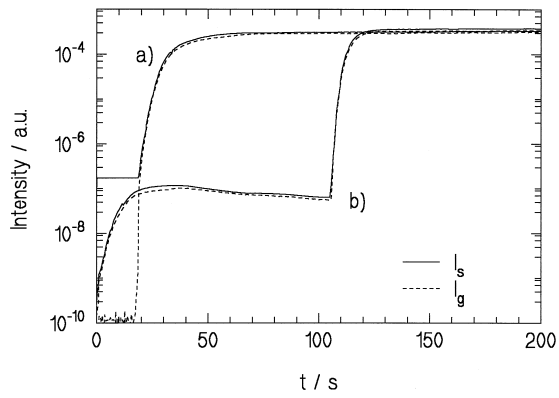

Fig. 2. Time evolution of the intensities of the signal beam I_s and the generated beam I_g for (a) switching on the pump beams after the signal beam and (b) vice versa.

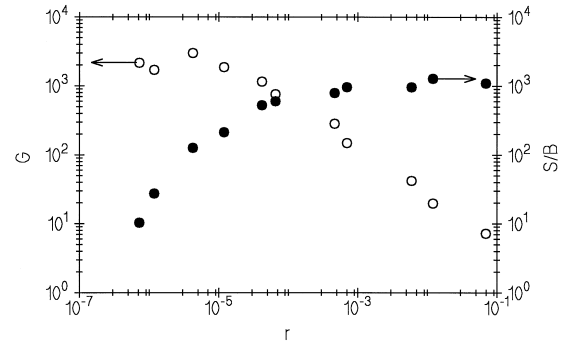

Fig. 3. Gain $G = I_s / I_s^i$ and signal-to-background ratio S/B as a function of the signal-to-pump ratio $r = I_s / (I_p^e + I_p^o)$.

additionally generated beam for both experiments. The intensity of this beam is practically equal to the signal beam intensity. Of course, no generated beam does exist without pump beams.

Fig. 3 shows the gain $G = I_s / I_s^i$ of the signal beam as a function of the signal-to-pump ratio $r = I_s^i / (I_p^o + I_p^e)$. I_s is the intensity of the transmitted and I_s^i of the incident signal beam. A maximum gain $G = 3000$ is reached for $r = 2 \times 10^{-6}$. We also plot the measured signal-to-background ratio $S/B = I_s / I_{scatt}$ at saturation as a function of r. Here I_{scatt} is the maximum scattering intensity which is responsible for the background with the proposed amplification process. The influence of beam-fanning can be neglected compared to parametric scattering. On the one hand, the signal beam propagates in a direction of low fanning, on the other hand, the ordinary pump beam reduces the beam-fanning [14].

To demonstrate image amplification we insert a lens (focal length 200 mm) and an amplitude transparency (grating) in the path of the expanded signal beam. First the crystal is located close to the focal plane of the lens. The photograph in Fig. 4(a) shows a segment of the scattering cone. The regions of the signal beam corresponding to wavevectors that fulfill Eq. (1) are amplified, whereas the other regions are not. Where the cone crosses the signal beam it is amplified by a factor of 9000. The photo in Fig. 4(b) shows the corresponding region of the generated beam where the amplified parts of the signal wave are observed, too. In a second experiment we locate the transparency close to the sample input face and project the amplified image to the photocamera with the help of a lens put after the sample. An amplified image of the grating recorded in such a way is shown in Fig. 4(c).

From Fig. 4(a) we infer that the spatial-frequency spectrum of the image to be amplified is strongly restricted in the vertical direction, whereas there are only slight restrictions along the cone (horizontal direction). To study this we measure the angular bandwidth of the gain. The dots in Fig. 5 show a vertical scan of the transmitted signal intensity shown in Fig. 4(a), whereas the squares corre-

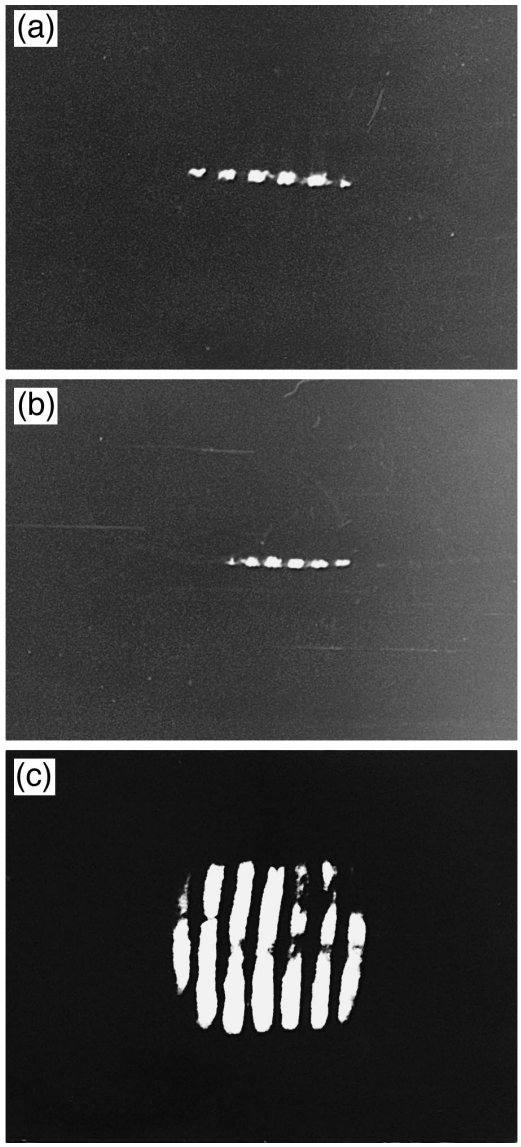

Fig. 4. Demonstration of image amplification: (a) Region of the amplified signal beam on the scattering cone with an amplitude transparency (grating) in the path of the expanded signal beam. (b) Corresponding region of the generated beam on the scattering cone. (c) Amplified image (see text).

spond to a scan on the cone in the horizontal direction as a function of the azimuth angle φ (see Fig. 1(a)). We made both measurements without the transparency containing the grating in the signal beam path. The curves represent the calculated dependences given in the following section. The measured angular bandwidth $\Delta\Theta_s = 1.5$ mrad in the vertical direction limits the spatial-frequency spectrum in this direction to 3 lines/mm, whereas we observe within the measured angular deviations no changes of the gain in the horizontal direction (see Fig. 5).

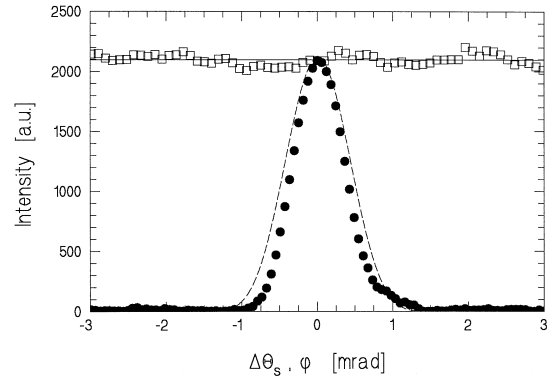

Fig. 5. Measurement of the spatial bandwidth: Vertical (●) and horizontal (□) scan of the transmitted signal intensitiy. The dashed curve represents the intensity as a function of the angular divergency $\Delta\Theta_s$ from exact phase matching. The solid curve corresponds to the variation of the gain with the azimuth angle φ.

Working with the lens positioned in the signal wave in front of the input face of the sample we are able to check the phase conjugate nature of the generated wave. If the crystal is located before the focal plane of the lens, i.e. the signal beam converges inside the sample, the generated wave becomes divergent. If, on the contrary, the lens is repositioned in such a way that the signal wave diverges inside the sample it is seen that the generated wave is converging at a certain plane after the sample. That means, the sign of curvature of the generated spherical wave just at the output face of the sample is always opposite to the sign of curvature of the signal wave.

3. Theory

The description of this process can be deduced from the theory of the corresponding scattering process given in the Refs. [4,10]. The amplitudes $A_{s,g}$ of the signal and generated beam for propagation in the direction of highest gain, i.e. $\varphi = 0$ in Fig. 1(a), read in the undepleted pump approximation and for $(\Gamma - \alpha)l \gg 1$:

$$A_s(x=l) = \tfrac{1}{2} A_s(x=0)\exp((\Gamma-\alpha)l/2),$$
$$A_g(x=l) = \tfrac{1}{2} A_s^*(x=0)\exp(i\Phi)\exp((\Gamma-\alpha)l/2). \quad (2)$$

Here $l = 3.2$ mm is the interaction length, $\Phi = \Phi_p^o + \Phi_p^e$ is the sum of the phases of the two pump beams, and $*$ denotes complex conjugation. The exponential gain factor for the intensity reads [4,10]

$$\Gamma = \frac{\pi}{\lambda\cos\theta_s}\,\frac{\sqrt{I_p^e I_p^o}}{I_p^o + I_p^e}\, n^3 r_{42}\,(\boldsymbol{E}\cdot\boldsymbol{e}_s^o), \quad (3)$$

with the electrooptic coefficient r_{42}, the space charge field

$$\boldsymbol{E} = \left(\boldsymbol{e}_{\mathrm{p}}^{\mathrm{o}} \cdot \boldsymbol{e}_{\mathrm{s}}^{\mathrm{o}}\right) \frac{k_{\mathrm{B}}T}{e} \frac{\boldsymbol{K}}{1 + \boldsymbol{K} \cdot \hat{\boldsymbol{\epsilon}} \cdot \boldsymbol{K}\, \epsilon_0\, k_{\mathrm{B}}T/N_{\mathrm{eff}}e^2}, \qquad (4)$$

the grating wave vector $\boldsymbol{K} = \boldsymbol{k}_{\mathrm{p}}^{\mathrm{o}} - \boldsymbol{k}_{\mathrm{s}}^{\mathrm{o}}$ and the polarization vectors of the ordinary polarized pump and signal wave $\boldsymbol{e}_{\mathrm{p,s}}^{\mathrm{o}}$ (inside the crystal). Here T denotes the absolute temperature, k_{B} the Boltzmann constant, N_{eff} the effective number of traps, $\epsilon_0\hat{\boldsymbol{\epsilon}}$ the dielectric tensor and e the absolute value of the electron charge.

We derive from Eq. (2) that the amplitude of the generated beam is proportional to the phase-conjugate signal amplitude, i.e., the generated beam is a forward phase-conjugate beam. Because of this a converging signal beam causes a diverging generated wave and vice versa. Additionally the generated beam $\boldsymbol{k}_{\mathrm{g}}^{\mathrm{o}}$ contains the signal beam information with the wavevectors $\boldsymbol{k}_{\mathrm{s}}^{\mathrm{o}}$ that fulfill Eq. (1), as can be seen in the photograph of Fig. 4(b).

According to Eq. (2) the intensities of both beams should be equal as measured in the experiment and shown in Fig. 2. When we take into account the finite trap density [15] ($N_{\mathrm{eff}} = 10^{16}$–$10^{17}$ cm^{-3}) we calculate for $r_{42} = 1640$ pm/V and $2\theta_{\mathrm{p}} = 48°$ an exponential gain factor Γ = (14–82) cm^{-1}. Both, the measured signal beam gain G = 3000 (Fig. 3) corresponding to $\Gamma = 33$ cm^{-1} and the measured image amplification ($G = 9000$) corresponding to $\Gamma = 37$ cm^{-1}, are in agreement with theory. They are equivalent to $N_{\mathrm{eff}} = 3 \times 10^{16}$ cm^{-3}. The difference in the two experimental values can be explained by an angular deviation from exact phase matching in the beam amplification experiment due to inprecise adjustment.

Next we include a small phase mismatch $\Delta\boldsymbol{k}$ in the theory. The phase-matching conditions are violated and Eq. (1) becomes $\boldsymbol{k}_{\mathrm{p}}^{\mathrm{o}} + \boldsymbol{k}_{\mathrm{p}}^{\mathrm{e}} = \boldsymbol{k}_{\mathrm{s}}^{\mathrm{o}} + \Delta\boldsymbol{k} + \boldsymbol{k}_{\mathrm{g}}^{\mathrm{o}}$. The solution for the signal amplitude then becomes

$$A_{\mathrm{s}}(x = l) = \tfrac{1}{2} A_{\mathrm{s}}(x = 0) \frac{\Gamma}{\sqrt{\Gamma^2 - \Delta k_x^2}} \times \sinh\left(\sqrt{\Gamma^2 - \Delta k_x^2}\, l/2\right) \exp(-\mathrm{i}\Delta k_x\, l/2). \qquad (5)$$

The dashed curve in Fig. 5 represents the dependence according to Eq. (5) with a gain factor $\Gamma = 37$ cm^{-1}, fitting well the experimental values. The spatial-frequency spectrum of the image is limited to 3 lines/mm in the vertical direction.

A variation of the azimuth angle φ (see Fig. 1(a)) preserves the phase-matching conditions but reduces the exponential gain factor. The solid curve in Fig. 5 corresponds to the theoretical dependence $\Gamma \propto \sqrt{0.516 - \sin^2\varphi}$ for $\theta_{\mathrm{p}} = 24°$ given in Ref. [4]. It becomes important only for large azimuth angles ($\varphi >$ 0.1 rad). Because of this no limitations within the measured angular deviations (Fig. 5) are observed. For this reason the proposed amplification process is best suited for one-dimensional images, e.g. gratings.

4. Conclusions

In summary, we present a new method of light amplification in photorefractive $BaTiO_3$. Our experiments prove for the first time that photorefractive parametric amplification processes may be utilized for the amplification of coherent light beams. We observe beam gains up to 3000 with a signal-to-background ratio S/B > 100 and demonstrate image amplification up to a factor of 9000. Because there exist 19 different parametric amplification processes [16] for two pump waves, further improvements should be possible. As a consequence of the phase-matching conditions involved our amplification process is appropriate for one-dimensional images.

Acknowledgements

We thank B.I. Sturman for helpful discussions. Financial support of the Deutsche Forschungsgemeinschaft (SFB 225, D9) is gratefully acknowledged.

References

[1] R.A. Rupp, F.W. Drees, Appl. Phys. B 39 (1986) 223.
[2] D.A. Temple, C. Warde, J. Opt. Soc. Am. B 3 (1986) 337.
[3] M. Ewbank, P. Yeh, J. Feinberg, Optics Comm. 59 (1986) 423.
[4] S. Odoulov, B. Sturman, L. Holtmann, E. Krätzig, Appl. Phys. B 52 (1991) 317.
[5] M. Horowitz, B. Fischer, Optics Lett. 17 (1992) 1082.
[6] J. Neumann, G. Jäkel, E. Krätzig, Optics Lett. 20 (1995) 1531.
[7] Y. Fainman, E. Klancnik, S.H. Lee, Opt. Eng. 25 (1986) 228.
[8] T. Tschudi, A. Herden, J. Goltz, H. Klumb, F. Laeri, J. Albers, IEEE J. Quantum Electron. QE-22 (1986) 1493.
[9] S. Breugnot, H. Rajbenbach, M. Defour, J.-P. Huignard, Optics Lett. 20 (1995) 447.
[10] S. Odoulov, B.I. Sturman, JETP 75 (1992) 447.
[11] B. Sturman, S. Odoulov, L. Holtmann, U. van Olfen, Appl. Phys. A 55 (1992) 65.
[12] S. Breugnot, D. Dolfi, H. Rajbenbach, J.-P. Huignard, Optics Lett. 19 (1994) 1070.
[13] L. Holtmann, E. Krätzig, S. Odoulov, Appl. Phys. B 53 (1991) 1.
[14] Q.P. He, P. Yeh, Appl. Optics 33 (1994) 283.
[15] P. Günter, J.-P. Huignard (Eds.), Photorefractive Materials and Their Applications I, Springer, Berlin, 1988.
[16] B.I. Sturman, S.G. Odoulov, M.Yu. Goulkov, Phys. Rep. 275 (1996) 197.